

Nafion-Sulfonated Poly(arylene ether sulfone) Composite Membrane for Direct Methanol Fuel Cell

Jisu Choi, Il Tae Kim, and Sung Chul Kim*

*Center for Advanced Functional Polymers, Department of Chemical and Biomolecular Engineering,
Korea Advanced Institute of Science and Technology, Daejeon 305-701, Korea*

Young Taik Hong

Korea Research Institute of Chemical Technology, Daejeon 305-600, Korea

Received August 24, 2005; Revised October 19, 2005

Abstract: Composite membranes of Nafion and sulfonated poly(arylene ether sulfone) were prepared. Sulfonated poly(arylene ether sulfone)s with different degrees of sulfonation were blended with Nafion to reduce the methanol crossover. The morphology, proton conductivity and methanol permeability of the resulting composite membranes were investigated by SEM, EDAX, AC impedance spectroscopy and permeability measuring instrument. The cross-sections of the composite membranes showed a phase separated morphology. The morphology and phase separation mechanism could be controlled by varying the blend ratio and the degree of sulfonation of poly(arylene ether sulfone). These complex morphologies can be applied for reducing methanol crossover. The methanol permeability and proton conductivity of the composite membranes were lower than those of Nafion 117 membrane since the development of an ionic pathway in the blend membrane was more difficult than that in Nafion itself.

Keywords: sulfonated poly(arylene ether sulfone), Nafion, blend, PEM, DMFC.

Introduction

Fuel cell is an energy conversion device, which converts chemical energy directly into electrical energy with high efficiency and low emission of pollutants. Fuel cell technology is expected to become one of the key technologies of the 21st century because the fuel utilization in fuel cell engines is markedly higher than in combustion engines.¹ While hydrogen is the best fuel in terms of operating the fuel cell itself, its production, storage and distribution are complicated. Alternatively liquid fuels that can produce hydrogen are utilized, like gasoline or methanol. Direct methanol fuel cell (DMFC) attracted interest for the mobile and domestic application due to low operating temperature, fast start-up and easy fuel storage and transportation. Methanol is easily obtained from natural source, it has a high specific energy density, it is liquid at operating temperature and, most of all, the existing infrastructure for transporting petroleum may easily be transformed to methanol transport.^{2,3} DMFC systems are based on a solid polymer electrolyte membrane, which not only transports dissolved reactants (protons) but also provides a physical barrier to prevent the mixing of the

fuel and oxidant gas.⁴ The commercially available polymer electrolyte membranes are not optimized for the DMFC. Although Nafion membranes show excellent properties in hydrogen fuel cells (high proton conductivity, good mechanical and thermal stability), they are not suitable for DMFC applications due to the high methanol permeability. Methanol permeation (methanol crossover) wastes fuel and causes significant loss of performance at the cathode. A number of approaches have been taken to reduce the methanol crossover in the DMFC including modified perfluorinated materials,^{5,6} sulfonated polyhydrocarbons,⁷⁻¹¹ acid-base blends with a surplus of acid ionic groups,^{12,13} and inorganic-organic composite materials.¹⁴⁻¹⁶

In this study, we prepared composite membranes consisting Nafion and poly(arylene ether sulfone). Poly(arylene ether sulfone)s with varying degree of sulfonation were blended with Nafion as a methanol barrier layer. Poly(arylene ether sulfone) shows lower methanol permeability than Nafion and good chemical and mechanical stability.¹⁷⁻¹⁹ The aim of this work is to reduce the methanol crossover by obstructing the ionic clusters of Nafion membrane which are responsible for the methanol crossover.

*Corresponding Author. E-mail: kimsc@kaist.ac.kr

Experimental

Materials. Nafion[®] solution (20 wt%, EW 1000, sulfonic acid form) in 1-propanol, ethanol and water mixture were purchased from E. I. Dupont de Nemours & Co.. Nafion solution was used as received. Sulfonated poly(arylene ether sulfone)s were synthesized from commercially available 4,4'-dichlorodiphenylsulfone (DCDPS) and 4,4'-biphenol obtained from BP Amoco and Eastman Chemical, respectively. The sulfonated comonomer, 3,3'-disulfonate-4,4'-dichloro-diphenylsulfone (SDCDPS) was synthesized from DCDPS according to a modified literature method. A general synthesis of the copolymers is shown in Figure 1.¹⁷⁻¹⁹ Sulfonated poly(arylene ether sulfone) will be abbreviated to PSSf-XX where XX is the degree of sulfonation. NMP, DMSO and other solvents were purchased from Aldrich and used as received.

Film Preparation. Solution blends of Nafion and poly(arylene ether sulfone) were prepared by the following procedure. At first, poly(arylene ether sulfone) powder was dissolved in NMP (13 wt%), and the appropriate Nafion solution in NMP (13 wt%) was added to the dissolved solution. Co-solvents of Nafion, water and alcohols, were substituted by NMP before blending. The solution blends were vigorously stirred and cast onto the glass substrate then dried in a convection oven for 12 h at 100 °C and 12 h at 140 °C to remove NMP completely.

Characterization

FTIR. FTIR spectroscopy was used to confirm the pendant functional groups on the copolymers. The spectra were recorded in the absorption mode on a Bomem-MB 100 FTIR spectrometer with thin, homogeneous cast films.

NMR. Structures and the degree of sulfonation of synthesized sulfonated poly(arylene ether sulfone) were confirmed by ¹H NMR that was recorded by Bruker AMX 500 spectrometer with DMSO.

Thermal Analysis. The glass transition temperatures (T_g) were obtained on a TA instruments' differential scanning

calorimeter (DSC) Q100. Scans were conducted under nitrogen at a heating rate of 10 °C/min. The thermal stabilities were measured on a TA instruments' thermogravimetric analysis (TGA) Q 500. The typical heating rate was 10 °C/min under air.

Water Uptake. The amount of water absorbed in membranes was determined by the following procedure; the wet membranes were vacuum-dried at 100 °C for 24 h, weighed and immersed in deionized water at room temperature for 24 h. The wet membranes were wiped dry and quickly weighed again. The water uptake was reported in weight percent: water uptake = $(W_{wet} - W_{dry}) / W_{dry} \times 100$ where W_{wet} and W_{dry} were the weights of the wet and dry membranes, respectively.

Ion Exchange Capacity. Ion exchange capacities (IEC) of polymers were determined by titration. The sulfonated poly(arylene ether sulfone) solutions in DMAC were titrated by standard tetramethyl ammonium hydroxide solution (~0.05 N, in iso-propanol). One sharp end point was confirmed the strong acid (-SO₃H) base reaction.

Electron Microscopy. The morphology of the membrane was investigated by scanning electron microscopy (SEM, JSM 5610) and energy dispersive X-ray analysis (EDAX, Philips, Phoenix). All the specimens were sputter-coated with gold. Morphology was analyzed by image analyzer (LEICA Qwin Standard)

Proton Conductivity. The proton conductivity of the membrane samples were measured by the AC impedance spectroscopy technique over a frequency range 0.1-10 MHz with AC perturbation of 10 mV, using Solatron 1255 frequency response analyzer. The conductivity σ of the sample was calculated from the impedance data, using the relation $\sigma = d/S \cdot R$ where d and S are the thickness and area of the electrode respectively, and R was derived from the impedance data.

Methanol Permeability. A glass cell with double baths was used to measure the permeability of the membranes. Initially, One bath was filled with methanol solution (5 wt% in deionized water), and the other with pure deionized water to reproduce a phenomenon of methanol crossover in DMFC system. The membrane was clamped between these two baths and the solution in each bath was stirred with magnetic stirrer during measurement. The methanol concentration in the methanol bath as a function of time (t) can be expressed by

$$C_B(t) = S \cdot D \cdot K \cdot C_{A_0} \frac{(t - t_0)}{V_B \cdot L} \quad (1)$$

where C_{A_0} is the initial concentration of methanol, L membrane thickness, S surface area, V_B volume of deionized water bath. Methanol diffusivity and sorption coefficient of the membrane are named as D and K , respectively. The methanol permeability can be obtained from the product D and K , which is calculated from the regressed slope of $C_B(t)$

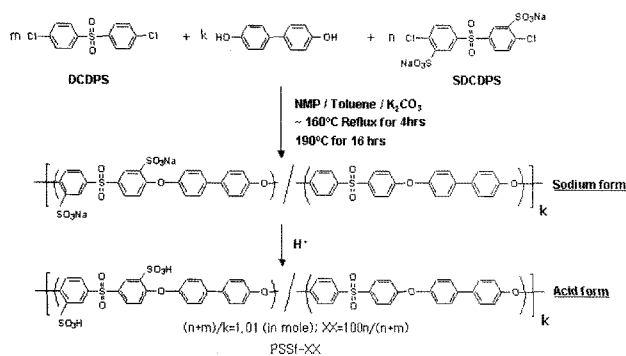


Figure 1. Synthesis of sulfonated poly(arylene ether sulfone).

vs. time (t) of methanol permeation according to the eq. (1). Sample solution was withdrawn from the bath by a microsyringe and analyzed by the Abbe Refractometer.

Results and Discussion

Characteristics of the Sulfonated Poly(arylene ether sulfone). The successful introduction of sodium sulfonate groups was confirmed by FTIR spectra (Figure 2). The characteristic peaks at 1030 cm^{-1} assigned to symmetric stretching of the sodium sulfonate groups were observed for all sulfonated copolymers (PSSf-20, PSSf-40). The intensity of these two peaks increased with higher degree of sulfonation. The degree of sulfonation could be calculated by NMR analysis. The calculated degree of sulfonation from NMR spectrum was in good agreement with the expected value. This result proved that the sulfonate groups were quantitatively introduced to the copolymer. The characteristics of the sulfonated poly(arylene ether sulfone)s are summarized in Table I. The introduction of sulfonate groups increased the glass transition temperatures (T_g) due to the increased intermolecular interaction by pendant ionic group and bulkiness of the pendant group. The thermal stabilities of sulfonated copolymers in sodium form were investigated by TGA. The temperature where rapid weight loss is observed is defined as the thermal decomposition tempera-

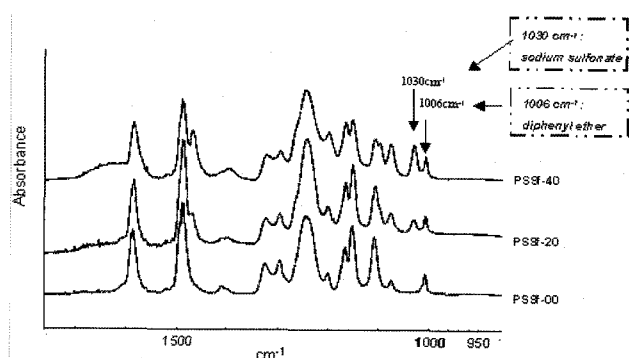


Figure 2. FTIR spectra of sulfonated poly(arylene ether sulfone).

Table I. Characteristics of Sulfonated Poly(arylene ether sulfone)

	PSSf-00	PSSf-20	PSSf-40
T_g (°C)	221	246	271
$T_{decomposition}$ (°C)	631	568	531
Cal. IEC (meq/g)	0	0.12	1.7
Exp. IEC (meq/g)	0	0.088	1.6
Water uptake (%)	3.4	9.8	28
Proton conductivity (S/cm)	-	1.15×10^{-3}	4.08×10^{-3}
Methanol permeability (cm^2/s)	-	4.25×10^{-8}	1.89×10^{-7}

ture (T_d). Poly(arylene ether sulfone) is a well known thermally stable polymer and shows higher T_d than that of Nafion (457°C). The T_d decreased with the increase of degree of sulfonation. All the experimental ion exchange capacity (IEC) values were in good agreement with the calculated IECs, confirming that sodium sulfonate could be introduced into polymer via sulfonated monomers without any side reactions, which were often observed in post-sulfonation methods. The IEC values increased with the increase in the degree of sulfonation. Water uptake in weight percent increased with increasing sulfonate content due to the strong hydrophilicity of the sulfonate groups. The proton conductivities and methanol permeabilities of the sulfonated copolymers were measured in fully hydrated condition at room temperature. The proton conductivity increased with increasing the sulfonate content reaching $4.08 \times 10^{-3}\text{ S/cm}$ with 40 mole% of the sulfonated comonomer. The proton conductivity of PSSf-40 is about 1/3 of the Nafion conductivity. The methanol permeability also increased with increasing the sulfonated content. PSSf-40 has methanol permeability about 1/7 of the Nafion.

Ternary System of Nafion/PSSf/NMP. The phase diagrams of Nafion/PSSf/NMP at room temperature were investigated to ascertain the mechanisms of phase separation. From Figure 3(A), we could find that the blend solution of Nafion and PSSf-00 (13 wt%) was miscible while the blend solutions of Nafion and PSSf-20 or PSSf-40 (13 wt%) were immiscible. The miscibility between Nafion and PSSf-00 was higher than those of Nafion and PSSf-20 or PSSf-40. The PSSf-20 and PSSf-40 have polar sulfonate group in the main chain, but Nafion has hydrophobic backbone with polar sulfonate group in the side chain, which may be the cause of the immiscibility. In the case of PSSf-20 and PSSf-40, two-layers of PSSf rich top layer and Nafion rich bottom layer were observed while PSSf-00/Nafion blend formed homogeneous solution at room temperature. Nafion rich phase formed the bottom layer since the specific gravity of Nafion (1.75-1.85) was much higher than that of PSSf (1.2-1.3). The phase diagrams of Nafion/PSSf-20/NMP and the Nafion/PSSf-40/NMP were very similar. To investigate the temperature effect on the miscibility between Nafion and PSSf, the phase diagrams of high temperature (at 68°C) were measured. The phase diagrams are shown in Figure 3(B). In the case of blend system of Nafion and PSSf, the temperature effect was not very significant on the miscibility between Nafion and PSSf.

Morphology. The morphology of the composite membrane is shown in Figure 4. The SEM morphology revealed that liquid-liquid phase separation between Nafion and PSSf occurred during the evaporation of NMP. The morphology of composite membranes using PSSf-20 and PSSf-40 shows two-layer structure with PSSf-rich top layer and Nafion-rich bottom layer. This is due to the high density of Nafion rich liquid. Two-layer structure was not formed in

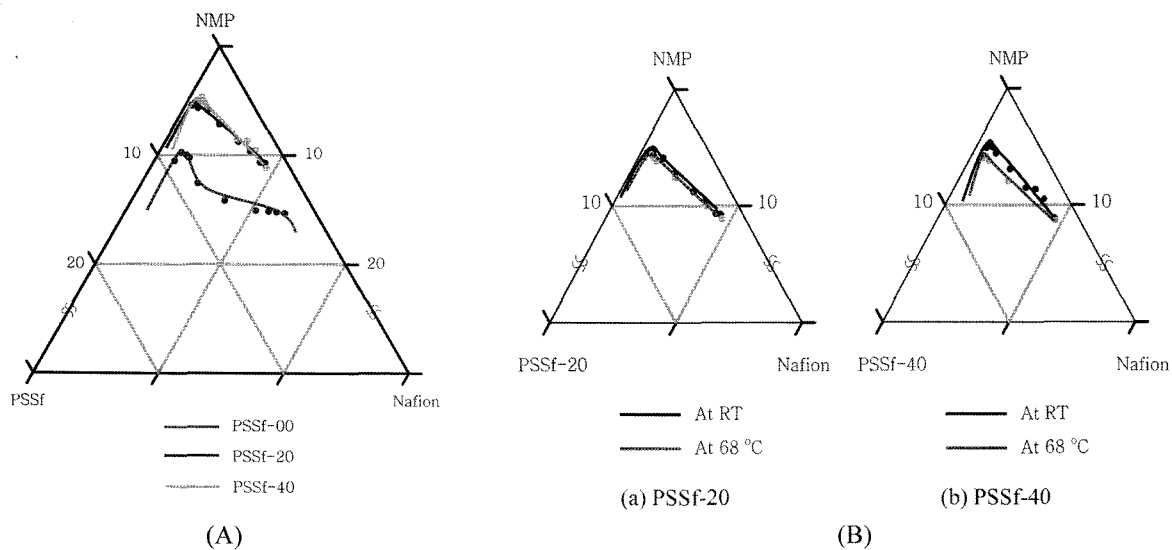


Figure 3. (A) Phase diagram of Nafion/PSSf (sodium form)/NMP at room temperature; (B) (a) Phase diagram of Nafion/PSSf-20/NMP and (b) Phase diagram of Nafion/PSSf-40/NMP.

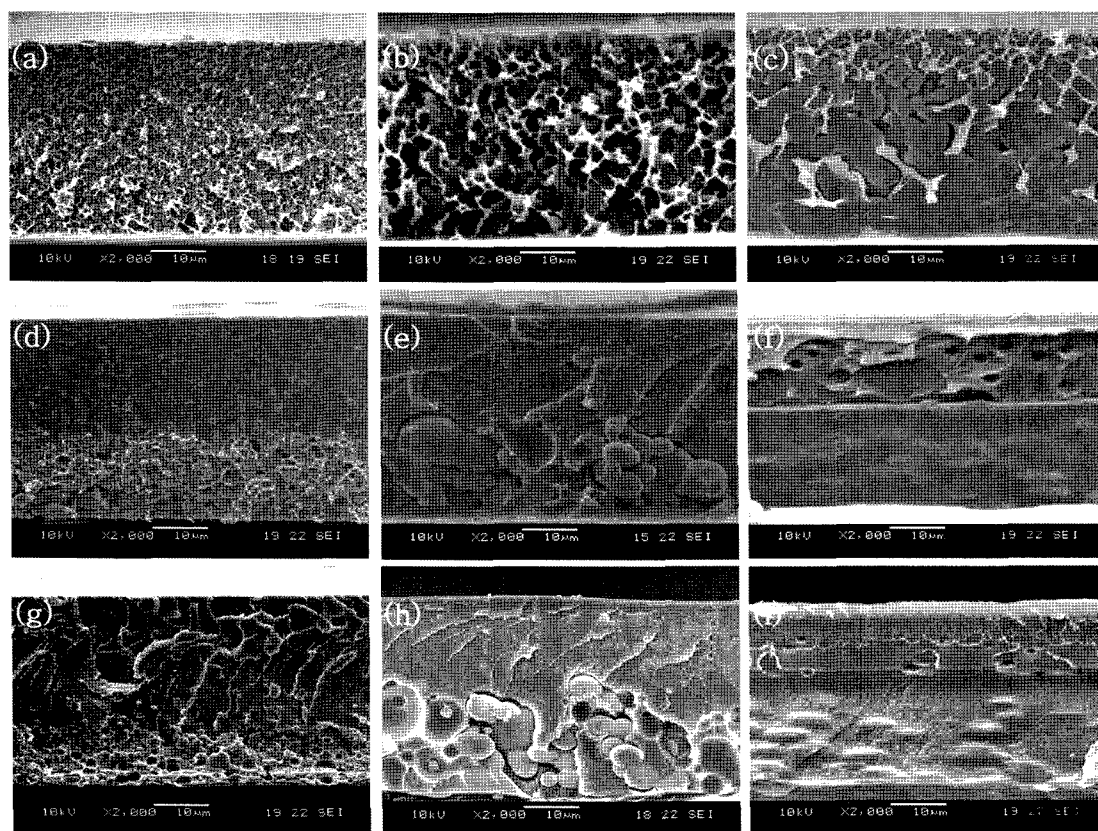


Figure 4. SEM micrographs of blend membranes: (a) PSSf-00:Nafion=2:1, (b) PSSf-00:Nafion=1:1, (c) PSSf-00:Nafion=1:2, (d) PSSf-20:Nafion=2:1, (e) PSSf-20:Nafion=1:1, (f) PSSf-20:Nafion=1:2, (g) PSSf-40:Nafion=2:1, (h) PSSf-40:Nafion=1:1, and (i) PSSf-40:Nafion=1:2

PSSf-00/Nafion blend because the phase separation started to occur at later stage of solvent evaporation due to the rela-

tively better miscibility of PSSf-00/Nafion and the high viscosity of the phase separated liquid prevented the

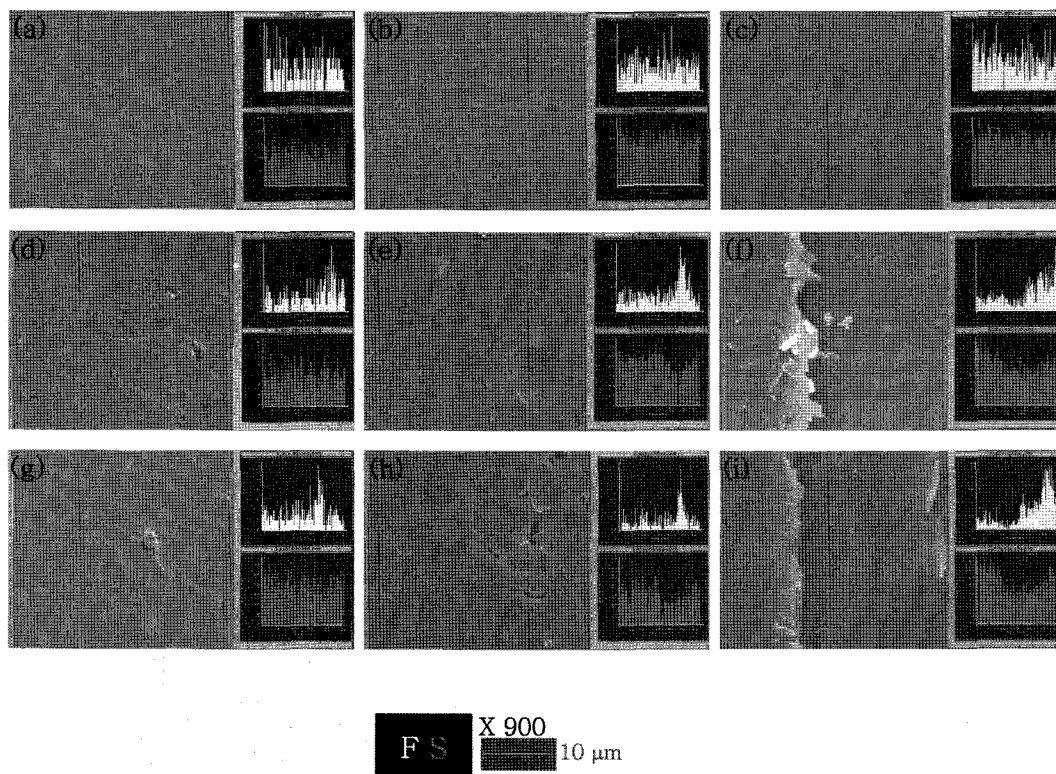


Figure 5. EDAX micrographs of blend membranes: (a) PSSf-00:Nafion=2:1, (b) PSSf-00:Nafion=1:1, (c) PSSf-00:Nafion=1:2, (d) PSSf-20:Nafion=2:1, (e) PSSf-20:Nafion=1:1, (f) PSSf-20:Nafion=1:2, (g) PSSf-40:Nafion=2:1, (h) PSSf-40:Nafion=1:1, and (i) PSSf-40:Nafion=1:2.

coalescence of the domains to form two-layer structure. In this case, spinodal decomposition occurred in the whole layer and co-continuous morphology was formed. We could confirm that fluorine elements of Nafion were dispersed in the whole layer from the EDAX results as shown in Figure 5. The phase separation mechanism of PSSf-20/Nafion and PSSf-40/Nafion blend is two-step. Firstly, two layers were formed. One is PSSf rich top layer and the other is Nafion rich bottom layer. When cast onto the glass plate, Nafion rich liquid layer was settled in the bottom side because the specific gravity of Nafion was much higher than that of PSSf. In PSSf rich top layer, nucleation and growth mechanism occurred as the secondary phase separation as NMP evaporated further and sea-island morphology was formed with PSSf matrix and Nafion domain. The morphology of Nafion rich bottom layer was changed with blend composition. In the case of higher content of Nafion, the secondary phase separation in the Nafion rich bottom layer occurred with nucleation and growth mechanism and PSSf formed domains in Nafion matrix as shown in Figure 4(f) & (i). In the case of higher content of PSSf, the content of PSSf is high in Nafion rich bottom layer and the secondary phase separation occurred with spinodal decomposition and co-continuous morphology was formed. From the EDAX results shown in Figure 5, the distribution of Nafion in the

membrane was confirmed. This complex morphology can be applied in reducing the methanol crossover in DMFC system. Top layer with PSSf matrix can reduce the methanol crossover and bottom layer with Nafion matrix can enhance the proton conduction.

Proton Conductivity and Methanol Permeability. Proton conductivity and methanol permeability of blend membrane are summarized in Table II. The methanol permeability of blend membrane was much lower than that of Nafion because PSSf acted as the methanol barrier. It increased with increasing the Nafion content in blend solution and increasing the degree of sulfonation of PSSf. The proton conductivity showed similar trend with the methanol permeability. The proton conductivity was also lower than that of Nafion 117 membrane. It increased with increasing the Nafion content in blend solution and increasing the degree of sulfonation of PSSf. The thickness of PSSf rich top layer and Nafion rich bottom layer are summarized in Table III. The thickness of PSSf rich top layer was 38-68% of total thickness of membrane. Due to this thick barrier layer, the proton conductivity of blend membrane was somewhat low. Proton conductivity could be enhanced by thinning PSSf rich top layer. Methanol permeability vs. proton conductivity is shown in Figure 6. To enhance the proton conductivity, the morphology of blend membranes

Table II. Methanol Permeability (a) and Proton Conductivity (b) of Blend Membranes

(a) Methanol Permeability of Blend Membranes

	PSSf:Nafion = 2:1	PSSf:Nafion = 1:1	PSSf:Nafion = 1:2
PSSf-00	1.74×10^{-8}	2.35×10^{-8}	3.22×10^{-8}
PSSf-20	6.91×10^{-8}	8.37×10^{-8}	9.90×10^{-8}
PSSf-40	1.27×10^{-7}	1.97×10^{-7}	3.26×10^{-7}

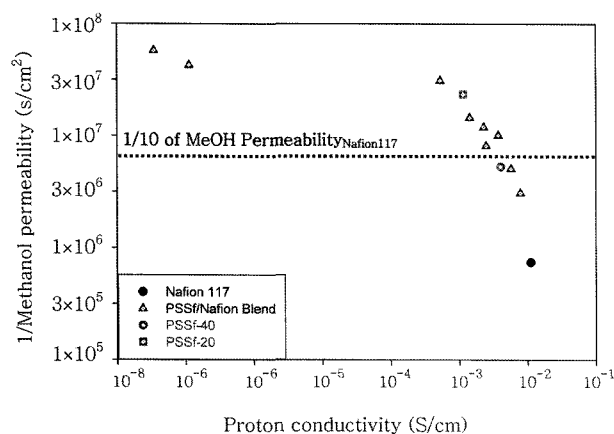
(cm²/s, Nafion 117: 1.34×10^{-6} cm²/s)

(b) Proton Conductivity of Blend Membranes

	PSSf:Nafion = 2:1	PSSf:Nafion = 1:1	PSSf:Nafion = 1:2
PSSf-00	3.48×10^{-8}	1.14×10^{-7}	5.31×10^{-4}
PSSf-20	1.43×10^{-3}	2.30×10^{-3}	3.75×10^{-3}
PSSf-40	2.48×10^{-3}	5.78×10^{-3}	7.91×10^{-3}

(S/cm, Nafion 117: 1.12×10^{-2} S/cm)**Table III. Thickness of PSSf Rich Top Layer and Nafion Rich Bottom Layer of Blend Membranes**

		PSSf:Nafion = 2:1	PSSf:Nafion = 1:1	PSSf:Nafion = 1:2
PSSf-00	Top	co-continuous	co-continuous	co-continuous
	Bottom			
PSSf-20	Top	20.00	18.57	14.29
	Bottom	14.28	17.14	17.14
PSSf-40	Top	21.43	19.29	12.86
	Bottom	10.00	16.43	21.43

Top : PSSf rich layer. Bottom : Nafion rich layer (μm).**Figure 6.** 1/Methanol permeability vs. proton conductivity.

could be varied by controlling the blend ratio or drying condition.

Conclusions

In this study Nafion/sulfonated poly(arylene ether sulfone) composite membranes for fuel cell were investigated. Sulfonated poly(arylene ether sulfone)s were successfully synthesized by direct polymerization using sulfonated comonomer. Modified Nafion membranes by solution blending with sulfonated poly(arylene ether sulfone) were prepared. The cross-sections of blend membranes showed phase separated morphologies. In case of PSSf-00, co-continuous morphology was formed. The phase separation mechanism of PSSf-20/Nafion and PSSf-40/Nafion blend occurs in two-step. Firstly, two layers were formed. One is PSSf rich top layer and the other is Nafion rich bottom layer. Secondary phase separation occurs during the NMP evaporation process and complex morphology is formed. These complex morphologies can be applied for reducing methanol crossover in DMFC. PSSf rich top layer can reduce the methanol crossover and Nafion rich bottom layer will improve the proton conduction. The methanol permeability and proton conductivity of blend membranes was lower than those of Nafion 117 membrane because the percolation of ionic pathway in blend membrane was more difficult than Nafion itself. To enhance the proton conductivity, the morphology of blend membranes could be varied.

Acknowledgements. The authors acknowledge LG Chem. Ltd. for the financial support.

References

- (1) J. Larminie and A. Dicks, *Fuel Cell Systems Explained*, John Wiley & Sons, 2000.
- (2) K. Kordesch and G. Simader, *Fuel Cells and Their Applications*, VCH, 1996.
- (3) L. Carrette and K. A. Friedrich, *Chemphyschem*, **1**, 162 (2000).
- (4) M. P. Walsh, *J. Power Sources*, **29**, 13 (1990).
- (5) B. Yang and Manthiram, *Electrochemistry Communication*, **6**, 231 (2004).
- (6) L. J. Hobson, H. Ozu, M. Yamaguchi, and S. Hayase, *J. Electrochem. Soc.*, **148**, A1185 (2001).
- (7) B. Baradie, C. Poinsingon, J. Y. Sanchez, Y. Piffard, G. Vitter, N. Bestaoui, D. Foscallo, A. Denoyelle, D. Delabouglise, and M. Vaujany, *J. Power Sources*, **74**, 8 (1998).
- (8) M. T. Bishop, F. E. Karasz, P. S. Russo, and K. H. Langley, *Macromolecules*, **18**, 86 (1985).
- (9) T. Kobayashi, M. Rikukawa, K. Sanui, and N. Ogata, *Solid State Ionics*, **106**, 219 (1998).
- (10) K. Miyatake, H. Iyotani, K. Yamamoto, and E. Tsuchida, *Macromolecules*, **29**, 6969 (1996).
- (11) X. Glipa, M. E. Haddad, D. J. Jones, and J. Rozière, *Solid State Ionics*, **97**, 323 (1997).
- (12) J. A. Kerres, A. Ullrich, F. Meier, and T. Häring, *Solid State Ionics*, **125**, 243 (1999).

- (13) J. A. Kerres, *J. Membrane Sci.*, **185**, 3 (2001)
- (14) A. S. Aricò, P. Creti, P. L. Antonucci, and V. Antonucci, *Electrochem. Solid. St.*, **1**, 66 (1998).
- (15) C. Yang, P. Costamagna, S. Srinivasan, J. Benziger, and A. B. Bocarsly, *J. Power Sources*, **103**, 1 (2001).
- (16) S. M. J. Zaidi, S. D. Mikhailenko, G. P. Robertson, M. D. Guiver, and S. Kaliaguine, *J. Membrane Sci.*, **173**, 17 (2000).
- (17) F. Wang, M. Hickner, Q. Ji, W. Harrison, J. Mechem, T. A. Zawodzinski, and J. E. McGrath, *Macromol. Symp.*, **175**, 387 (2001).
- (18) F. Wang, M. Hickner, Y. S. Kim, T. A. Zawodzinski, and J. E. McGrath, *J. Membrane Sci.*, **197**, 231 (2002).
- (19) Y. S. Kim, C. Dong, M. A. Hickner, T. E. Glass, V. Webb, and J. E. McGrath, *Macromolecules*, **36**, 17 (2003).